Geochemistry, Geophysics, Geosystems

Supporting Information for

Geochemical Evidence in the Northeast Lau Basin for Subduction of the Cook-Austral Volcanic Chain in the Tonga Trench

Allison A. Price*[1], Matthew G. Jackson[1], Janne Blichert-Toft[2], Jerzy Blusztajn[3] Christopher S. Conatser[4], Jasper G. Konter[5], Anthony A.P. Koppers[4], Mark D. Kurz[6]

1. University of California, Santa Barbara, Department of Earth Science, 1006 Webb Hall, Santa Barbara, CA, 93106 USA (*price@umail.ucsb.edu)

2. Laboratoire de Géologie de Lyon, CNRS UMR 5276, Ecole Normale Supériere de Lyon and Université Claude Bernard Lyon 1, 46 Allée d'Italie, 69007 Lyon, France

3. Department of Geology and Geophysics, Woods Hole Oceanographic Institution, Woods Hole, MA, USA

4. College of Earth, Ocean and Atmospheric Sciences, Oregon State University, 104 CEOAS Administration Building, Corvallis, Oregon 97331-5503, USA

5. Dept. of Geology and Geophysics, School of Ocean and Earth Science and Technology, University of Hawaii, Manoa, 1680 East-West Rd, Honolulu, HI 96822, USA

6. Department of Marine Chemistry, Woods Hole Oceanographic Institution, Woods Hole, Massachusetts, USA

*Corresponding author

Contents of this file

Text S1
Figures S1 and S2
Tables S1

Additional Supporting Information (Files uploaded separately)

Data sets S1 to S7

Introduction

In Text S1 we provide an in depth overview of the four mixing models that are discussed in Section 4.2 of the main text. For reference we also include plots of the new isotopic data presented in this study along with previously published lavas from the Lau Basin in Figures S1 and S2. Lastly, we provide a table of descriptions that briefly describes each of the rock samples used in this study.

Text S1.

1. Dredge-D44 lavas with a HIMU component

The first geochemically distinct group of lavas from dredge-D44, D44-HIMU, has the most radiogenic Pb isotopic ratios identified in the Lau Basin to date. In most isotopic spaces, lavas from the D44-HIMU group consistently plot in, or near, the field defined by Rurutu hotspot lavas (Figs. 5 and 6). Plots including $^{207}Pb/^{204}Pb$ show that, with the exception of the HIMU Rurutu hotspot, there are no mantle components in the region (including Samoa and Louisville) with sufficiently high $^{207}Pb/^{204}Pb$ to explain the radiogenic Pb isotopic compositions in D44-HIMU lavas. However, D44-HIMU lavas are geochemically enriched compared to the end-member HIMU Rurutu hotspot lavas by having higher $^{87}Sr/^{86}Sr$ (0.704080-0.704087) and lower $^{143}Nd/^{144}Nd$ (0.512778-0.512784). The only hotspots and volcanoes in the region exhibiting such enriched signatures include the Samoan shield and rejuvenated lavas, lavas from the Rarotonga hotspot, lavas from the Louisville hotspot, and lavas from nearby Uo Mamae seamount. We can exclude Rarotonga as the source of the enriched component because Rarotonga has low $^{207}Pb/^{204}Pb$ and the enriched component must have elevated $^{207}Pb/^{204}Pb$ (Fig. 6). Using plots including $\Delta^{207}Pb/^{204}Pb$ or $\Delta^{208}Pb/^{204}Pb$, defined in *Hart* [1984] (see caption of Fig. 6), we can also exclude Louisville as the origin of the enriched component. Louisville lavas have low $\Delta^{207}Pb/^{204}Pb$ while the enriched component requires higher $\Delta^{207}Pb/^{204}Pb$. Thus, only the enriched components from Uo Mamae and Samoa remain to explain the enriched mantle component needed to account for the low $^{143}Nd/^{144}Nd$ and high $^{87}Sr/^{86}Sr$ in D44-HIMU lavas. In a plot of $^{143}Nd/^{144}Nd$ versus $^{87}Sr/^{86}Sr$ (Fig. 5), the D44-HIMU lavas plot away from the field for Rurutu hotspot lavas and are shifted toward an EM1 component; D44-HIMU lavas plot below the shallow array formed by Samoan lavas. Uo Mamae hosts a clear EM1

signature [e.g., *Pearce* et al. 2007; *Regelous* et al. 2008] that also plots below the Samoan array (at lower $^{143}Nd/^{144}Nd$ for a given $^{87}Sr/^{86}Sr$) and therefore defines an end-member that can plausibly anchor the enriched component inferred for the D44-HIMU lavas. In all isotopic spaces, the D44-HIMU lavas plot between the fields for HIMU lavas in the Rurutu hotspot and Uo Mamae lavas. In Figs. 5 and 6 and Table 5, we present a mixing model that generates isotopic compositions similar to the D44-HIMU lavas when a Rurutu hotspot melt component (from the Arago and ZEP2-12 seamounts, but related to the Rurutu hotspot; *Bonneville* et al. [2006]) is mixed with a melt from Uo Mamae. The mixing model does a reasonable job of capturing the isotopic compositions in the D44-HIMU lavas in all isotopic spaces. Other volcanoes from the Rurutu hotspot track do not act as appropriate end-members for this mixing model, and unfortunately there are no Hf isotopic data for Arago or the ZEP2-12 seamounts. Therefore, the mixing model (and subsequent mixing models for the other lavas in this study) is not evaluated in $^{176}Hf/^{177}Hf$ versus $^{143}Nd/^{144}Nd$ space. In summary, a mixture of a HIMU component from the Rurutu hotspot and an EM1 component from Uo Mamae (plausibly related to the Rarotonga hotspot, see section 4.1.1.) generates isotopic compositions that match many of the isotopic features observed in D44-HIMU lavas.

2. Dredge-D44 lavas with an enriched mantle (EM) component

The second geochemical group of lavas from dredge-D44, designated D44-EM, consists of boninite series lavas that have the highest $^{87}Sr/^{86}Sr$ in this study, but do not exhibit Pb isotopic ratios as high as the D44-HIMU lavas (Fig. 5). D44-EM lavas still have relatively high $^{207}Pb/^{204}Pb$ (up to 15.642) and are shifted toward a component with relatively high $^{206}Pb/^{204}Pb$ and $^{208}Pb/^{204}Pb$, such as Rurutu or Louisville, in all isotopic spaces. However, Rurutu represents a more plausible HIMU end-member for D44-EM lavas than the Louisville: mixtures of Louisville with other possible end-member components in the region do not consistently reproduce isotopic compositions similar to those in D44-EM. In plots using Sr and Nd isotopic ratios versus $^{207}Pb/^{204}Pb$, the D44-EM lavas fall in the field defined by lavas from the Rurutu hotspot (Fig. 6), and elevated $^{207}Pb/^{204}Pb$ in the D44-EM lavas provides a powerful constraint for the origin of the

radiogenic Pb isotopic (HIMU) signature in the D44-EM lavas and suggests an origin in the Rurutu hotspot. However, like D44-HIMU lavas, in multiple isotopic spaces D44-EM samples are shifted away from the field of Rurutu lavas toward a second component with an enriched mantle composition with higher $^{87}Sr/^{86}Sr$, lower $^{143}Nd/^{144}Nd$, and lower $^{206}Pb/^{204}Pb$. However, there are only a few non-Rurutu volcanoes and hotspots in the region with geochemically enriched $^{87}Sr/^{86}Sr$ as high as that observed in D44-EM lavas which plausibly could have contributed to the Lau Basin mantle: the Samoa and Rarotonga hotspots and Uo Mamae seamount. Again, a plot of $^{87}Sr/^{86}Sr$ versus $^{143}Nd/^{144}Nd$ (Fig. 5) shows that D44-EM lavas trend away from Rurutu toward a component with high $^{87}Sr/^{86}Sr$ at a given $^{143}Nd/^{144}Nd$, which is similar to rejuvenated lavas found in Samoa. This contrasts with the EM1 component suggested for D44-HIMU lavas, which trend away from the Rurutu field toward a component (with lower $^{143}Nd/^{144}Nd$ at a given $^{87}Sr/^{86}Sr$) like that found in Uo Mamae. However, Samoa has a variety of geochemical components [*Jackson* et al. 2014], but in all isotopic spaces investigated here (in particular in $\Delta^{207}Pb/^{204}Pb$ versus $^{143}Nd/^{144}Nd$; Fig. 6), D44-EM samples trend toward the Samoa rejuvenated field. In Figs. 5 and 6 and Table 5, we present a mixing model that generates isotopic compositions similar to the D44-EM lavas by mixing a Rurutu hotspot component with a Samoan rejuvenated lava component. These models show that a mixture of a HIMU component from the Rurutu hotspot (i.e., lavas from Rurutu Island) and an enriched mantle component from a Samoan rejuvenated melt can generate isotopic compositions that approximate the D44-EM lavas in all isotopic spaces. A Samoan hotspot signature (entrained by toroidal flow) in the Lau Basin mantle, and a subducted HIMU component (either from subducted seamounts and volcanoclastic material with compositions similar to that identified in the Rurutu hotspot), are required to match the composition of D44-EM lavas.

3. Dredge-D44 lava with a depleted mantle, high $^{3}He/^{4}He$ component

The D44-depleted sample is the only lava from the present sample suite with high $^{3}He/^{4}He$ (19.3 Ra), a signature that has been observed previously in the Lau Basin

and is attributed to the incorporation of a high $^{3}He/^{4}He$ Samoan plume component in the Lau Basin [e.g. *Poreda and Craig* 1992; *Hilton* et al. 1993; *Honda* et al. 1993; *Lupton* et al. 2009; *Hahm* et al. 2012; *Lupton* et al. 2012]. The isotopic compositions of this lava are relatively well matched by mixing a geochemically depleted melt from the Lau Basin (similar in composition to depleted lavas from the ELSC; *Escrig* et al. [2009]; *Hergt and Woodhead* [2007]) with a shield component similar to the Samoan island of Ofu, the island with the highest $^{3}He/^{4}He$ (33.8 Ra) from the Samoan hotspot [*Jackson* et al., 2007; *Jackson* et al., 2009; *Hart and Jackson* 2014]. This mixing model (see Table 5 and Figs. 5 and 6) provides a reasonably good fit for this sample in multi-isotope space.

4. Dredge-D42 lavas

Dredge-D42 lavas also exhibit relatively radiogenic Pb isotopic compositions compared to other Lau Basin lavas, but not as extreme as those in the D44-HIMU lavas (Figs. 5 and 6). However, the Rurutu hotspot is the only component in the region with $^{207}Pb/^{204}Pb$ higher than the dredge-D42 samples (Louisville has lower $^{207}Pb/^{204}Pb$ than dredge-D42 lavas), and a Rurutu hotspot component is also needed to generate the HIMU signatures in these lavas (Fig 6). Again, like the D44-HIMU and D44-EM lavas, the dredge-D42 samples are shifted away from the field of Rurutu lavas toward a component with an enriched mantle (EM) composition that, in this case, has lower $^{143}Nd/^{144}Nd$ and higher $\Delta^{207}Pb/^{204}Pb$ (Fig. 6). Only three possible mantle sources in the region (Samoa shield/rejuvenated, Niuafo'ou Island, and Uo Mamae) have $\Delta^{207}Pb/^{204}Pb$ that is sufficiently high to contribute to the enriched component in the source of dredge-D42 lavas. In $^{87}Sr/^{86}Sr$ versus $^{143}Nd/^{144}Nd$ space, dredge-D42 samples are shifted away from the Rurutu field on a steeply sloped trajectory that indicates the presence of a component with lower $^{143}Nd/^{144}Nd$ at a given $^{87}Sr/^{86}Sr$ than Samoa. In all isotopic spaces, this trajectory points clearly toward an EM1 component like that found at Uo Mamae. Our mixing model, which includes Rurutu and Uo Mamae components, consistently reproduces compositions that are similar to the new isotopic data for dredge-D42 lavas (see Table 5 and Figs. 5 and 6). In summary, in a similar fashion as for D44-HIMU lavas, a mixture of a HIMU component from the Rurutu hotspot and an

enriched mantle component from Uo Mamae (plausibly related to the Rarotonga hotspot) can generate the isotopic compositions identified in dredge-D42 lavas.

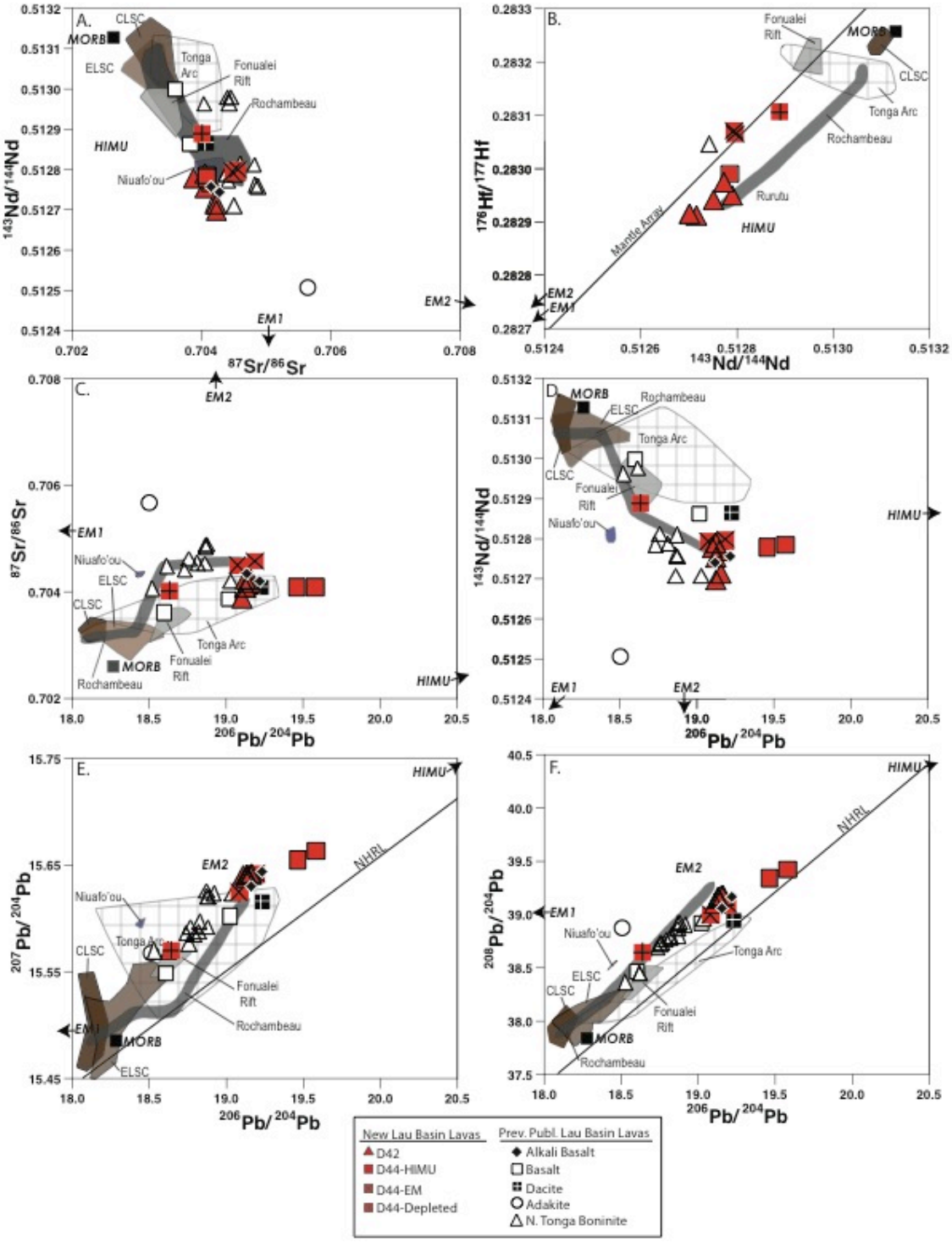

Figure S1. Figure S2. Sr, Nd, and Pb isotopic relationships among new lavas dredged from the NELB and other lavas from the Lau Basin. In addition to the new data from the NELB (plotted as various red symbols) previously published whole rock NELB lavas are shown as symbols. Data sources for figures S1 and S2 are the same. NELB data are from Falloon and Crawford [1991]; Danyushevsky et al. [1995]; Falloon et al. [2007]; Falloon et al. [2008], and Caulfield et al. [2012]. Rochambeau Bank and Rifts data are

from Volpe et al. [1988]; Poreda and Craig [1992]; Tian et al. [2011]; Lytle et al. [2012]. Fonualei Rift data are from Escrig et al. [2012]. Fonualei Rift is also known as the Fonualei Rift and Spreading Center (FRSC). Niuafo'ou data are from Regelous et al. [2008]; Tian et al. [2011]. Tonga Arc data are from Hergt and Woodhead [2007]; Turner et al. [2012]; Escrig et al. [2012]; Caulfield et al. [2015]. CLSC data are from Volpe et al. [1988]; Boespflug et al. [1990]; Pearce et al. [2007]; Hergt and Woodhead [2007]. Data for the ELSC is from Hergt and Woodhead [2007] and Escrig et al. [2009].

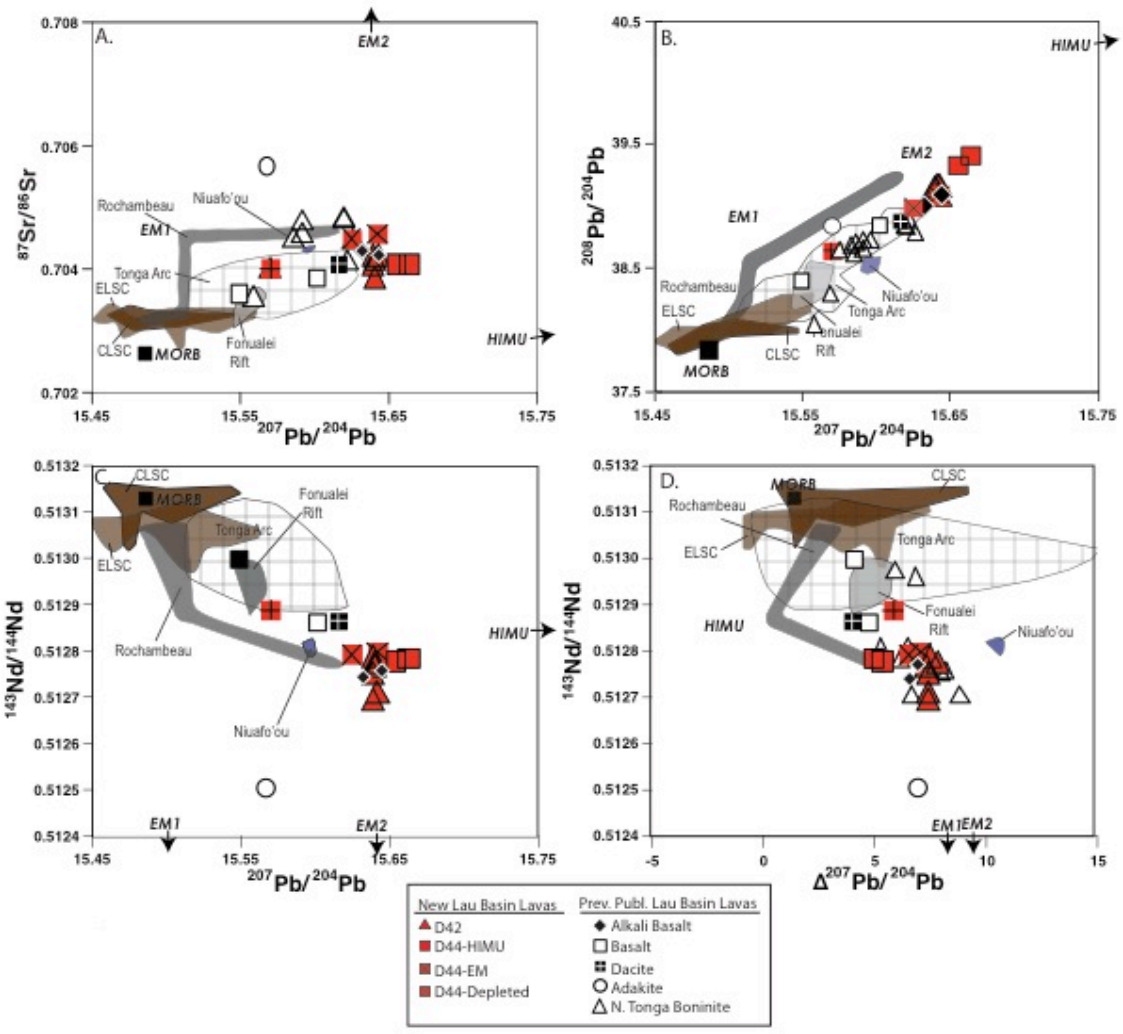

Figure S2. Sr, Nd, and Pb isotopic relationships among new lavas dredged from the NELB and other lavas from the Lau Basin. In addition to the new data from the NELB (plotted as various red symbols) previously published whole rock NELB lavas are shown as symbols. Data sources for figures S1 and S2 are the same. NELB data are from Falloon and Crawford [1991]; Danyushevsky et al. [1995]; Falloon et al. [2007]; Falloon et al. [2008], and Caulfield et al. [2012]. Rochambeau Bank and Rifts data are from Volpe et al. [1988]; Poreda and Craig [1992]; Tian et al. [2011]; Lytle et al. [2012]. Fonualei Rift data are from Escrig et al. [2012]. Fonualei Rift is also known as the Fonualei Rift and Spreading Center (FRSC). Niuafo'ou data are from Regelous et al. [2008]; Tian et al. [2011]. Tonga Arc data are from Hergt and Woodhead [2007]; Turner et al. [2012]; Escrig et al. [2012]; Caulfield et al. [2015]. CLSC data are from Volpe et al. [1988]; Boespflug et al. [1990]; Pearce et al. [2007]; Hergt and Woodhead [2007]. Data for the ELSC is from Hergt and Woodhead [2007] and Escrig et al. [2009].

Sample Name	Sample Description
D44-26	Magnesian andesite (with adakitic characteristics) with ~1% clinopyroxene phenocrysts (<1 mm). Minimally vesiculated (~2% subrounded vesicles ranging from 1-4 mm in diameter).
D44-15	Lava with ~20% clinopyroxene (~3 mm?) and resorbed olivine phenocrysts (3-8 mm) and ~15% subrounded vesicles ranging from 0.5-3 mm in diameter. Sample is altered and secondary alteration phases partially fill vesicles. Sample has a thin (<1 mm) ferromanganese crust. Due to alteration, isotopic measurements were carried out on clinopyroxene phenocrysts.
D44-38	Boninite with ~10% clinopyroxene and olivine phenocrysts ranging from 1-7 mm, vesiculated (~15% subrounded, elongate vesicles that are .25-5 mm in diameter).
D44-46	Boninite series lava with 5-10% clinopyroxene and olivine phenocrysts ranging from 1-5 mm. Sample is vesiculated, with ~3% subrounded, elongate vesicles ranging from ~1-25 mm in diameter.
D44-91	Tholeiite basalt. Minimally vesiculated with <1% highly spherical vesicles ranging from 0.25-1 mm in diameter; <1% olivine (<1 mm); glassy rind.
D42-60	Trachybasalt with 1% plagioclase phenocrysts (ranging from 1-10 mm) and vesiculated (~10% elongate, subrounded vesicles ranging from 1-10 mm length). 60% of vesicles host accessory sulfides.
D42-25	Alkali basalt with <1% plagioclase and olivine phenocrysts (~1 mm), vesiculated (~20% moderately spherical vesicles ranging from 0.25-3 mm in diameter) and 2 mm ferromanganese rind.
D42-05	Alkali basalt with ~1% plagioclase phenocrysts (1-5 mm length), vesiculated (~20% subangular vesicles that are ~1 mm in diameter). 1 mm coating of ferromanganese crust.
D42-30	Trachy-basalt with <1% olivine phenocrysts (1-2 mm), vesiculated (~10% subrounded vesicles, 1-6 mm in diameter). 5% of vesicles are completely filled with secondary alteration phases. 20% of vesicles host sulfides.
D42-20	Alkali basalt with <1% plagioclase and olivine phenocrysts (1-2 mm) and vesiculated (~10% subrounded vesicles ranging from 1-15 mm in diameter). 25% of vesicles are completely filled with secondary alteration phases.
D42-26 xenolith	Fresh olivine websterite xenolith (~60% orthopyroxene, 26% olivine, 10% clinopyroxene, and 4% spinel) nodule hosted in alkali basalt.

Table S1. Rock descriptions of samples analyzed in this study.

Data Set S1. Age dating data for sample D44-12.

Data Set S2. Age dating data for sample D44-26.

Data Set S3. Age dating data for sample D42-68.

Data Set S4. Age dating data for sample D42-67.

Data Set S5. Age dating data for sample D42-60.

Data Set S6. Age dating data for sample D44-08.

Data Set S7. Age dating data for sample D42-02.

References.

Boespflug X, Dosso L, Bougault H, Joron J (1990) Trace Element and Isotopic (Sr, Nd) Geochemistry of Volcanic Rocks from theLau Basin. Geologisches Jahrbuch Reihe D Heft 92 1–14.

Bonneville A, Dosso L, Hildenbrand A (2006) Temporal evolution and geochemical variability of the South Pacific superplume activity. Earth and Planetary Science Letters 244:251–269. doi: 10.1016/j.epsl.2005.12.037

Caulfield J, Blichert-Toft J, Albarede F, Turner S (2015) Corrigendum to "Magma evolution in the primitive, intra-oceanic Tonga arc: Petrogenesis of Basaltic Andesites at Tofua Volcano" and 'Magma evolution in the Primitive, Intra-oceanic Tonga arc: Rapid Petrogenesis of Dacites at Fonualei Volcano'. Journal of petrology 1–1.

Danyushevsky, L. V., Sobolev, A. V., & Falloon, T. J. (1995). North Tongan high-Ca boninite petrogenesis: the role of Samoan plume and subduction zone-transform fault transition. *Journal of Geodynamics*, *20*(3), 219-241.

Escrig S, Bézos A, Goldstein SL, et al. (2009) Mantle source variations beneath the Eastern Lau Spreading Center and the nature of subduction components in the Lau basin–Tonga arc system. Geochemistry Geophysics Geosystems 10:Q04014. doi: 10.1029/2008GC002281

Escrig S, Bézos A, Langmuir CH, et al. (2012) Characterizing the effect of mantle source, subduction input and melting in the Fonualei Spreading Center, Lau Basin: Constraints on the origin of the boninitic signature of the back-arc lavas. Geochemistry Geophysics Geosystems 13:n/a–n/a. doi: 10.1029/2012GC004130

Falloon TJ, Danyushevsky LV, Crawford TJ, et al. (2007) Multiple mantle plume components involved in the petrogenesis of subduction-related lavas from the

northern termination of the Tonga Arc and northern Lau Basin: Evidence from the geochemistry of arc and backarc submarine volcanics. Geochemistry Geophysics Geosystems 8:Q09003. doi: 10.1029/2007GC001619

Falloon, T. J., Danyushevsky, L. V., Crawford, A. J., Meffre, S., Woodhead, J. D., & Bloomer, S. H. (2008). Boninites and adakites from the northern termination of the Tonga Trench: implications for adakite petrogenesis. *Journal of Petrology*, *49*(4), 697-715.

Falloon, T. J., & Crawford, A. J. (1991). The petrogenesis of high-calcium boninite lavas dredged from the northern Tonga ridge. *Earth and Planetary Science Letters*, *102*(3), 375-394.

Hahm D, Hilton DR, Castillo PR, et al. (2012) An overview of the volatile systematics of the Lau Basin " Resolving the effects of source variation, magmatic degassing and crustal contamination. Geochimica et Cosmochimica Acta 85:88–113. doi:

Hart S (1984) A large-scale isotope anomaly in the Southern Hemisphere mantle. Nature 309:753–757.

Hart, S. R., & Jackson, M. G. (2014). Ta'u and Ofu/Olosega volcanoes: the "Twin Sisters" of Samoa, their P, T, X melting regime, and global implications.*Geochemistry, Geophysics, Geosystems*, *15*(6), 2301-2318.

Hergt J, Woodhead JD (2007) A critical evaluation of recent models for Lau–Tonga arc–backarc basin magmatic evolution. Chemical Geology 245:9–44. doi: 10.1016/j.chemgeo.2007.07.022

Hilton DR, Hammerschmidt K, Loock G, Friedrichsen H (1993) Helium and argon isotope systematics of the central Lau Basin and Valu Fa Ridge: Evidence of crust/mantle interactions in a back-arc basin. Geochimica et Cosmochimica Acta 57:2819–2841.

Honda M, Patterson DB, McDougall I, Falloon TJ (1993) Noble gases in submarine pillow basalt glasses from the Lau Basin: Detection of a solar component in backarc basin basalts. Earth and Planetary Science Letters 120:135–148.

Jackson MG, Hart SR, Konter JG, et al. (2014) Helium and lead isotopes reveal the geochemical geometry of the Samoan plume. Nature 514:355–358. doi: 10.1038/nature13794

Jackson MG, Kurz M, Hart S, Workman RK (2007) New Samoan lavas from Ofu Island reveal a hemispherically heterogeneous high $^{3}He/^{4}He$ mantle. Earth and Planetary Science Letters 264:360–374. doi: 10.1016/j.epsl.2007.09.023

Jackson, M. G., Kurz, M. D., & Hart, S. R. (2009). Helium and neon isotopes in phenocrysts from Samoan lavas: Evidence for heterogeneity in the terrestrial high 3 He/4 He mantle. *Earth and Planetary Science Letters*, *287*(3), 519-528.

Lupton JE, Arculus RJ, Greene RR, et al. (2009) Helium isotope variations in seafloor basalts from the Northwest Lau Backarc Basin: Mapping the influence of the Samoan hotspot. Geophysical Research Letters. doi: 10.1029/2009GL039468

Lupton JE, Arculus RJ, Jenner FE, Greene RR (2012a) Helium Isotope Variations in the Northern Lau and North Fiji Basins. In: AGU. pp V23B–2820

Lytle ML, Kelley KA, Hauri EH, et al. (2012) Tracing mantle sources and Samoan influence in the northwestern Lau back-arc basin. Geochemistry Geophysics Geosystems 13:n/a–n/a. doi: 10.1029/2012GC004233

Pearce JA, Kempton PD, Gill JB (2007) Hf-Nd evidence for the origin and distribution of mantle domains in the SW Pacific. Earth and Planetary Science Letters 260:98–114.

Poreda RJ, Craig H (1992) He and Sr isotopes in the Lau Basin mantle: depleted and primitive mantle components. Earth and Planetary Science Letters 113:487–493.

Regelous M, Turner S, Falloon TJ, et al. (2008) Mantle dynamics and mantle melting beneath Niuafo'ou Island and the northern Lau back-arc basin. Contributions to Mineralogy and Petrology 156:103–118. doi: 10.1007/s00410-007-0276-7

Tian L, Castillo PR, Hilton DR, et al. (2011) Major and trace element and Sr-Nd isotope signatures of the northern Lau Basin lavas: Implications for the composition and dynamics of the back-arc basin mantle. Journal of geophysical Research 116:B11201. doi: 10.1029/2011JB008791

Turner S, Caulfield J, Rushmer T, et al. (2012) Magma evolution in the primitive, intra-oceanic Tonga arc: rapid petrogenesis of dacites at Fonulaei volcano. Journal of petrology 53:1231–1253.

Volpe AM, Macdougall JD, Hawkins JW (1988) Lau Basin basalts (LBB): trace element and Sr-Nd isotopic evidence for heterogeneity in backarc basin mantle. Earth and Planetary Science Letters 90:174–186.